A sulfated carbohydrate epitope inhibits axon regeneration after injury

Joshua M. Brown[a,1], Jiang Xia[a,1], BinQuan Zhuang[a], Kin-Sang Cho[b], Claude J. Rogers[a], Cristal I. Gama[a], Manish Rawat[a], Sarah E. Tully[a], Noriko Uetani[c], Daniel E. Mason[d], Michel L. Tremblay[c], Eric C. Peters[d], Osami Habuchi[e], Dong F. Chen[b,f], and Linda C. Hsieh-Wilson[a,2]

[a]Division of Chemistry and Chemical Engineering and Howard Hughes Medical Institute, California Institute of Technology, Pasadena, California 91125; [b]Schepens Eye Research Institute, Massachusetts Eye and Ear, Department of Ophthalmology, Harvard Medical School, Boston, MA 02114; [c]The Goodman Cancer Center, McGill University, Montreal, Quebec H3A 1A3, Canada; [d]Genomics Institute of the Novartis Research Foundation, San Diego, California 92121; [e]Department of Chemistry, Aichi University of Education, Igaya-cho, Kariya, Aichi 448-8542, Japan; and [f]Veterans Affairs Boston Healthcare System, 150 South Huntington Avenue, Boston, Massachusetts 02130

Edited* by Peter G. Schultz, The Scripps Research Institute, La Jolla, CA, and approved January 23, 2012 (received for review December 27, 2011)

Chondroitin sulfate proteoglycans (CSPGs) represent a major barrier to regenerating axons in the central nervous system (CNS), but the structural diversity of their polysaccharides has hampered efforts to dissect the structure-activity relationships underlying their physiological activity. By taking advantage of our ability to chemically synthesize specific oligosaccharides, we demonstrate that a sugar epitope on CSPGs, chondroitin sulfate-E (CS-E), potently inhibits axon growth. Removal of the CS-E motif significantly attenuates the inhibitory activity of CSPGs on axon growth. Furthermore, CS-E functions as a protein recognition element to engage receptors including the transmembrane protein tyrosine phosphatase PTPσ, thereby triggering downstream pathways that inhibit axon growth. Finally, masking the CS-E motif using a CS-E-specific antibody reversed the inhibitory activity of CSPGs and stimulated axon regeneration in vivo. These results demonstrate that a specific sugar epitope within chondroitin sulfate polysaccharides can direct important physiological processes and provide new therapeutic strategies to regenerate axons after CNS injury.

A major obstacle to functional recovery after CNS injury is the inhibitory environment encountered by regenerating axons. Chondroitin sulfate (CS) polysaccharides and their associated proteoglycans (CSPGs) are the principal inhibitory components of the glial scar, which forms after neuronal damage and acts as a barrier to axon regeneration (1–3). It is well established that the inhibitory activity of CSPGs is derived from their CS chains, as chondroitinase ABC (ChABC) treatment promotes axon regeneration, sprouting, and functional recovery after injury in vivo (4–6). However, the mechanisms by which CS polysaccharides inhibit axon growth are poorly understood. Dissection of the structural determinants and mechanisms underlying CS activity is essential for understanding the barriers to axon regeneration and for developing new treatments to promote regeneration and functional recovery after spinal cord and other CNS injuries.

CS polysaccharides are composed of repeating disaccharide units, which undergo regiochemical sulfation during development and after injury (7–10). The CS-A (GlcA-4SGalNAc), CS-C (GlcA-6SGalNAc), and CS-E (GlcA-4S,6SGalNAc) disaccharides represent major sulfation motifs in the mammalian CNS (Fig. S1). Although the diverse patterns of CS polysaccharides lie at the heart of their biological activity, these complex sulfation patterns have also hampered efforts to understand the biological functions of CS. For example, genetic approaches are challenged by the presence of multiple sulfotransferase isoforms with overlapping specificities, and deletion of a single sulfotransferase gene can propagate global changes throughout the carbohydrate chain. The structural complexity of CS has also thwarted biochemical efforts to isolate well-defined, sulfated molecules. As such, only heterogeneous mixtures or purified samples biased toward abundant, readily isolable sequences have been available for biological investigations. Although studies have suggested that the CS-A, CS-E, and CS-C motifs are upregulated after neuronal injury and may play roles in axon regeneration (7, 9, 11), only heterogeneous polysaccharides were utilized for those studies, and there has been conflicting data, confounding the question of whether specific sulfation sequences are important. Indeed, because of the lack of structure-activity relationships, relatively nonspecific mechanisms have also been proposed, such as those brought about by steric blockage of the extracellular space (12), arrays of negatively charged sulfate (7), or obstruction of substrate adhesion molecules (13).

Here, we exploited chemically synthesized CS oligosaccharides and glycopolymers to examine systematically the role of specific sulfation sequences in axon regeneration. Our studies demonstrate that the CS-E sulfation motif is a key structural determinant responsible for the inhibitory activity of CSPGs. Moreover, we provide mechanistic insights into how CS-E enables CSPGs to inhibit axon growth through the identification of a specific neuronal receptor for CS-E. Finally, we show that blocking the inhibitory CS-E sugar motif can reverse CSPG-mediated inhibition and promote axon regeneration in vivo, providing a unique therapeutic approach to neural regeneration.

Results and Discussion

CS-E-Enriched Polysaccharides Inhibit Neurite Outgrowth and Repel Axons. To understand the role of specific sulfation motifs, we used CS polysaccharides enriched in particular motifs and exploited our ability to chemically synthesize defined CS-A, CS-C, and CS-E oligosaccharides. First, we compared the inhibitory effects of CSPGs and CS polysaccharides enriched in CS-A, CS-C, or CS-E disaccharide units on neurite outgrowth. Neurite outgrowth of dissociated dorsal root ganglion (DRG) neurons was inhibited by 58% of untreated control levels when grown on CSPGs (Fig. 1*A*). ChABC digestion largely abolished the effects, confirming the importance of the CS chains. CS polysaccharides enriched in the CS-E motif potently inhibited neurite outgrowth to approximately 50% of untreated control levels as suggested previously (7) and in a dose-dependent manner (Fig. 1 *A* and *B*). In contrast, polysaccharides enriched in the CS-A or CS-C motif had no appreciable effects on neurite outgrowth at the same glucuronic acid concentrations. The lack of inhibition observed for CS-A and

Author contributions: J.M.B., J.X., B.Z., and L.C.H.-W. designed research; J.M.B., J.X., B.Z., K.-S.C., C.J.R., C.I.G., S.E.T., and D.E.M. performed research; M.R., S.E.T., N.U., M.L.T., and O.H. contributed new reagents/analytic tools; J.M.B., J.X., B.Z., K.-S.C., C.J.R., C.I.G., D.E.M., E.C.P., D.F.C., and L.C.H.-W. analyzed data; and J.M.B., B.Z., D.F.C., and L.C.H.-W. wrote the paper.

The authors declare no conflict of interest.

*This Direct Submission article had a prearranged editor.

[1]These authors contributed equally to this work.

[2]To whom correspondence should be addressed. E-mail: lhw@caltech.edu.

This article contains supporting information online at www.pnas.org/lookup/suppl/doi:10.1073/pnas.1121318109/-/DCSupplemental.

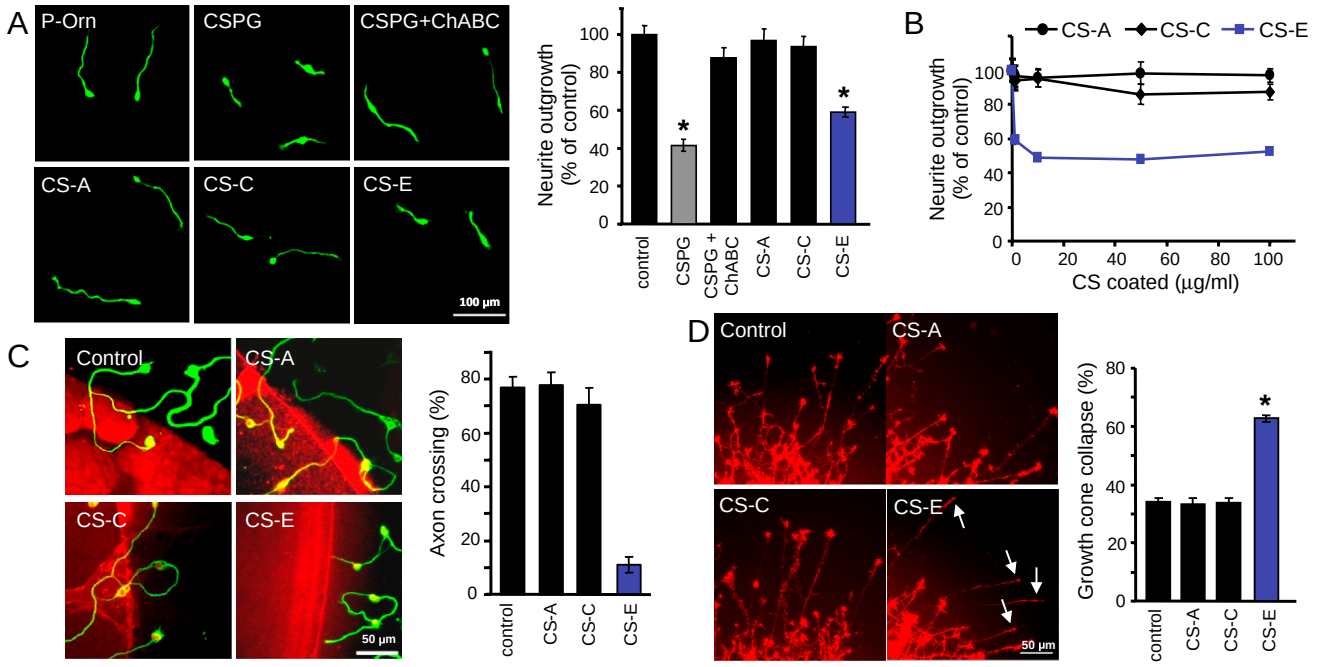

Fig. 1. CS-E-enriched polysaccharides inhibit DRG neurite outgrowth and induce growth cone collapse. (*A*) Dissociated chick E7 DRGs were cultured on a substratum of poly-DL-ornithine (P-Orn control), CSPGs, chondroitinase ABC-treated CSPGs, or CS polysaccharides enriched in the CS-A, CS-C, or CS-E sulfation motifs. Representative images and quantitation of average neurite length (±SEM, error bars) from three experiments ($n = 50–200$ cells per experiment). (*B*) Polysaccharides enriched in the CS-E sulfation motif, but not the CS-A or CS-C motifs, inhibit DRG neurite outgrowth in a dose-dependent manner. (*C*) CS-E-enriched polysaccharides repel axon crossing in a boundary assay. Polysaccharides (1 mg/mL) or PBS control were mixed with Texas Red and spotted on P-Orn coated coverslips. Dissociated rat P5-9 CGN neurons were immunostained with an anti-βIII-tubulin antibody. Representative images and quantitation of percentage of axon crossing (±SEM, error bars) from two experiments ($n = 30–50$ axons per experiment). (*D*) CS-E-enriched polysaccharides induce growth cone collapse. DRG explants from chick E7-9 embryos were grown on a P-Orn/laminin substratum, treated with medium (control) or the indicated polysaccharides, and stained with rhodamine-phalloidin. Representative images and quantitation of growth cone collapse (±SEM, error bars) from five experiments ($n = 50–100$ growth cones per experiment). Arrows indicate collapsed growth cones. All statistical analyses were performed using the one-way ANOVA test (*$P < 0.0001$, relative to control).

CS-C, even when used at 100-fold higher concentrations than CS-E (Fig. 1*B*), suggests that the inhibitory activity of CS-E polysaccharides is not simply due to their high overall negative charge. Similar results were obtained with cerebellar granule neurons (CGNs; Fig. S2), whose neurite growth is inhibited by CSPGs (14).

As CSPGs in the glial scar form an inhibitory boundary to growing axons, we examined whether polysaccharides enriched in the CS-E sulfation motif could repel axons in a boundary assay. Like CSPGs (15), CS-E-enriched polysaccharides formed an inhibitory zone that was strongly repellent to CGN axons (Fig. 1*C*). In contrast, axons freely crossed into boundaries enriched in the CS-A or CS-C motifs. CS-A-enriched polysaccharides also exhibited repulsive behavior as reported (8), but much higher concentrations of sugar were required (Fig. S3*A*).

It is known that CSPGs can acutely collapse growth cones to form dystrophic axonal structures that no longer extend, thus leading to long-term inhibition of regrowth (16). To examine whether CS-E is involved in the acute phase of the inhibitory response, we performed growth cone collapse assays. Application of CS-E-enriched polysaccharides to DRG or CGN explants significantly increased the number of collapsed growth cones within minutes (Fig. 1*D* and Fig. S3*B*), whereas CS-A- and CS-C-enriched polysaccharides had no effect. Taken together, these results indicate that CS polysaccharides are sufficient to recapitulate the inhibitory effects of CSPGs on neurons, and this activity depends critically on the CS sulfation pattern.

Pure CS-E Potently Inhibits Neurite Outgrowth and Collapses Growth Cones. Although natural polysaccharides enriched in CS-E shed light on how specific sulfation motifs function in CSPG-mediated axon inhibition, these data should be interpreted cautiously because polysaccharides containing a single, pure sulfation sequence have not traditionally been isolated from natural sources, and thus the possibility that the inhibitory activity is due to minor, contaminating motifs cannot be eliminated. Indeed, about 40% of the CS-E-enriched polysaccharide contains other sulfation motifs, and rare sulfation sequences are likely to be biologically important, as in the case of heparan sulfate glycosaminoglycans (17). As such, the intrinsic structural complexity and heterogeneity of CS pose a major obstacle to understanding structure-activity relationships.

To overcome this problem, we synthesized homogeneously sulfated glycopolymers displaying only the CS-A, CS-C, or CS-E sulfation motifs (Fig. 2*A*). Norbornene-linked CS-A, CS-C, or CS-E disaccharides were polymerized using ruthenium-catalyzed ring-opening metathesis polymerization (ROMP) chemistry. This approach generates glycopolymers of pure, defined sulfation sequence with molecular weights and biological activities comparable to natural CS polysaccharides (18). Previously, we showed that these molecules were powerful tools to study the roles of specific CS motifs in promoting neurite outgrowth of developing hippocampal neurons (19). In the context of DRG neurons, glycopolymers containing pure CS-E inhibited neurite outgrowth, whereas those containing pure CS-A or CS-C had minimal activity (Fig. 2*B* and Fig. S4). Moreover, the monovalent CS-E disaccharide at the same uronic acid concentration did not inhibit neurite outgrowth, confirming that the multivalent presentation of CS-E is critical for biological activity. Similarly, we found that glycopolymers containing pure CS-E potently induced growth cone collapse in DRG explants (Fig. 2*C*), whereas CS-A or CS-C glycopolymers had no effect. As CS polysaccharides are found as a complex mixture of different sulfation patterns in vivo, we also examined the activity of a glycopolymer mixture. A 1:1 mixture of CS-A and CS-E glycopolymers had no further effects on neurite outgrowth compared to the pure CS-E glycopolymer alone, confirming that sulfated mixtures do not confer additional inhibitory properties (Fig. S5).

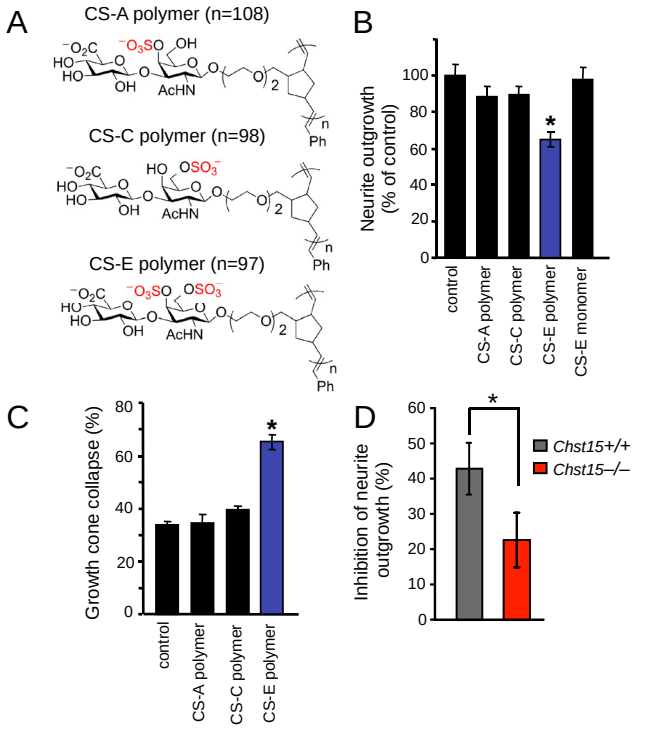

Fig. 2. The CS-E motif is a potent inhibitor of axon growth. (*A*) Structures of synthetic glycopolymers displaying pure CS-A, CS-C, and CS-E disaccharides. (*B*) The synthetic CS-E glycopolymer inhibits neurite outgrowth of chick E7 DRGs, whereas the CS-A glycopolymer, CS-C glycopolymer, and monovalent CS-E disaccharide have little effect. (*C*) The synthetic CS-E glycopolymer induces DRG growth cone collapse. (*D*) CSPGs from CS-E-deficient mice show significant loss of inhibitory activity on DRG neurite outgrowth. Mouse P8 DRGs were cultured on CSPGs purified from *Chst15* knockout or wild-type mice. Statistical analyses were performed using the one-way ANOVA test (*$P < 0.0001$, relative to control).

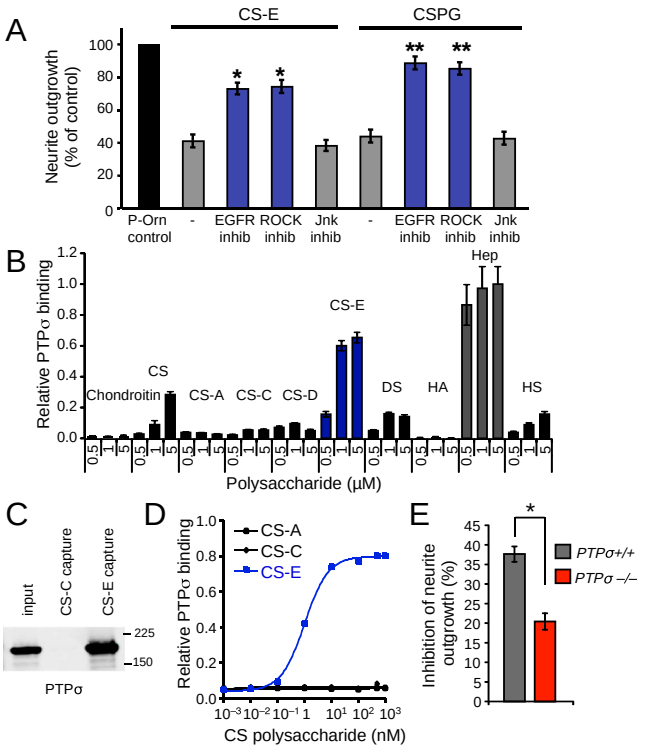

Fig. 3. The CS-E sulfation motif inhibits axon growth via PTPσ. (*A*) Inhibitors against EGFR (AG1478, 15 nM) and ROCK (Y27632, 5 μM) rescued CS-E- and CSPG-mediated inhibition of neurite outgrowth in dissociated rat P5-9 CGN cultures, whereas JNK inhibitor II (10 μM) had no effect. Quantitation of neurite outgrowth from three experiments is reported. (One-way ANOVA, *$P < 0.0001$, relative to CS-E control without inhibitors, **$P < 0.0001$, relative to CSPG control without inhibitors; $n = 50$–200 cells per experiment). (*B*) PTPσ binds selectively to CS-E-enriched polysaccharides on glycosaminoglycan microarrays. Microarrays were incubated with PTPσ-Fc, followed by a Cy3-conjugated antihuman IgG secondary antibody, and analyzed using a GenePix 5000a scanner. Graphs show quantification from three experiments ($n = 10$ per condition). (*C*) Coprecipitation of CS-E and PTPσ. Full-length PTPσ-mycHis was expressed in COS-7 cells and incubated with biotinylated CS-E or CS-C polysaccharides bound to streptavidin beads. PTPσ binding was detected by immunoblotting with an anti-myc antibody. (*D*) Specific, high affinity binding of CS-E polysaccharides to PTPσ. (*E*) *PTPσ* -/- neurons show significantly less inhibition by CS-E than wild-type control neurons. For each genotype, the percentage inhibition of neurite outgrowth is plotted relative to neurons treated with only P-Orn. Quantification from three experiments is shown. (One-way ANOVA, *$P < 0.005$, relative to control; n => 200 cells per experiment).

To complement our chemical approaches, we also investigated the contribution of the CS-E motif using genetic methods. We isolated CSPGs from mice containing a targeted gene disruption of *N*-acetylgalactosamine 4-sulfate 6-*O* sulfotransferase 15 (Chst15), the enzyme that generates CS-E via addition of a sulfate group to the 6-*O* position of GalNAc on CS-A (20). Consistent with potent inhibitory activity for CS-E, removal of CS-E from CSPGs resulted in significant loss of inhibitory activity on DRG neurite outgrowth (Fig. 2*D*). The remaining inhibitory effect of CSPGs from *Chst*$15^{-/-}$ mice is likely due to the proteoglycan core protein or other proteins in the mixture, as treatment with ChABC to remove CS chains did not reduce the inhibitory effects any further. Taken together, our chemical and genetic studies demonstrate conclusively that the CS-E motif is a potent inhibitor of axon growth and a critical inhibitory structure on CSPGs.

The CS-E Motif Activates Inhibitory Signaling Pathways. To investigate the molecular mechanisms by which CS-E inhibits axon growth, we examined the ability of CS-E to activate signaling pathways associated with inhibition of axon regeneration. CSPGs and myelin inhibitors have been shown to activate Rho/Rho-kinase (ROCK) and epidermal growth factor receptor (EGFR) pathways (8, 14, 15). Pharmacological inhibition of these signaling pathways effectively reversed the inhibitory effects of CSPGs on CGNs (Fig. 3*A* and Fig. S6). Specifically, the EGFR competitive inhibitor AG1478 and the ROCK inhibitor Y27632 restored neurite outgrowth to within 79–88% of untreated control levels, in agreement with previous studies (14, 15). Importantly, we found that the EGFR and ROCK inhibitors also neutralized the inhibitory activity of CS-E polysaccharides and rescued neurite outgrowth to a similar extent. In contrast, inhibition of c-Jun N-terminal kinase (JNK) pathways using JNK inhibitor II showed no effect on either CS-E- or CSPG-mediated neurite inhibition, as expected (15). Moreover, treatment of COS-7 cells with CS-E or CSPGs led to activation of RhoA (Fig. S7). Thus, CS-E activates intracellular signaling pathways involved in CSPG-mediated inhibition of axon regeneration, further supporting the notion that this sugar epitope is a major inhibitory component of CSPGs.

The CS-E Motif Inhibits Neurite Outgrowth via PTPσ. The ability of CS-E to trigger downstream signaling pathways suggests that CS-E may directly engage protein receptors at the cell surface, thereby initiating intracellular signaling. Recently, CSPGs were shown to interact with protein tyrosine phosphatase PTPσ, a transmembrane receptor known to bind heparan sulfate proteoglycans (21, 22). *PTPσ* gene disruption reduced axon inhibition by CSPGs in culture (22) and enhanced regeneration in sciatic, facial, optic, and spinal cord nerves in vivo (22–25). However, it remains unknown whether (and which) specific sulfation motifs on CS mediate the interactions of CSPGs with PTPσ.

In light of our results showing that CS-E is a major inhibitory motif on CSPGs, we examined the potential interaction between CS-E and PTPσ using carbohydrate microarrays (26). A soluble PTPσ-Fc fusion protein, but not other receptors such as EphA2-Fc or Fc alone, bound efficiently to CS-E polysaccharides arrayed on poly-lysine-coated glass slides (Fig. 3*B* and Fig. S8). PTPσ showed strong binding to heparin and CS-E polysaccharides, with weaker binding to chondroitin sulfate and dermatan sulfate (both of which contain some CS-E) and heparan sulfate. Little or no binding to CS-A, CS-C, or CS-D polysaccharides was observed, highlighting the specificity of PTPσ for the CS-E sulfation motif.

To confirm further the PTPσ-CS-E interaction, biotinylated CS-E or CS-C polysaccharides were conjugated to streptavidin beads and incubated with COS-7 cell lysates expressing full-length PTPσ. We found that CS-E polysaccharides were capable of pulling down PTPσ, whereas CS-C polysaccharides showed no interaction (Fig. 3*C*). In addition to this heterologous cell system, we captured PTPσ from a rat brain membrane protein-enriched fraction and identified the protein by mass spectrometry analysis (Fig. S9). Lastly, we showed that biotinylated CS-E, but not CS-A or CS-C, polysaccharides bind immobilized PTPσ with high affinity according to a Langmuir binding model (Fig. 3*D*). The apparent dissociation constant ($K_{D,\mathrm{app}}$) of approximately 1 nM is similar to values reported for the association of PTPσ with the CSPGs neurocan and aggrecan (22).

Having demonstrated that CS-E interacts specifically with PTPσ, we next tested whether CS-E and PTPσ form a functional association. Deletion of PTPσ significantly attenuated CS-E-induced inhibition of neurite outgrowth in DRG neurons (Fig. 3*E*), indicating that PTPσ is required for CS-E to inhibit neurite outgrowth. Interestingly, residual inhibition by CS-E (approximately 22%) remained in PTPσ-deficient neurons, consistent with previous observations with CSPGs (22). These results suggest that CS-E may also engage other receptors, possibly leukocyte common antigen-related phosphatase (LAR) (27) and as-yet-undiscovered receptors, although we cannot rule out additional receptor-independent mechanisms, such as charge repulsion or reduced cell adhesion. Together, these studies demonstrate that the fine structure of CS chains mediates interactions with receptors involved in axon regeneration, and they identify PTPσ as a critical functional receptor for CS-E.

Generation of a Selective CS-E Blocking Antibody. An important implication of these results is that blocking CS-E interactions may prevent the inhibition caused by CSPGs and promote axon regeneration. To generate a CS-E blocking agent, we raised a monoclonal antibody against a pure synthetic CS-E tetrasaccharide (28). Although antibodies have been generated previously using CS polysaccharides as antigens (29, 30), their specificity has been limited by the structural heterogeneity of natural polysaccharides. Synthetic chemistry has the advantage of providing defined molecules of precise sulfation sequence, which can be used as antigens, for screening antibodies, and for characterizing binding specificities. An antibody generated in this manner was highly selective for the CS-E sulfation motif, as measured by dot blot, ELISA, carbohydrate microarrays, and surface plasmon resonance (Fig. 4*A* and Figs. S10 and S11). Strong binding to pure CS-E tetrasaccharides and natural CS-E polysaccharides was observed, with minimal binding to CS-A or CS-C tetrasaccharides and other glycosaminoglycan classes. Notably, this antibody also bound a mixture of CSPGs derived from chick brain (Fig. 4*B*), confirming the presence of the CS-E epitope on CSPGs, and blocked the interaction of CS-E polysaccharides with PTPσ (Fig. S12).

CS-E Blocking Antibody Promotes Axon Regeneration. To test whether blocking the CS-E epitope reverses the inhibitory effects of CSPGs, we added the CS-E antibody to DRG neurons grown on a substratum of CSPGs. Neurite inhibition by CSPGs was significantly decreased by addition of the CS-E antibody, with neurite outgrowth returning to 79% of control levels (Fig. 4*C*). In contrast, neither a CS-A monoclonal antibody nor an IgG control antibody had any effect on CSPG-mediated neurite outgrowth.

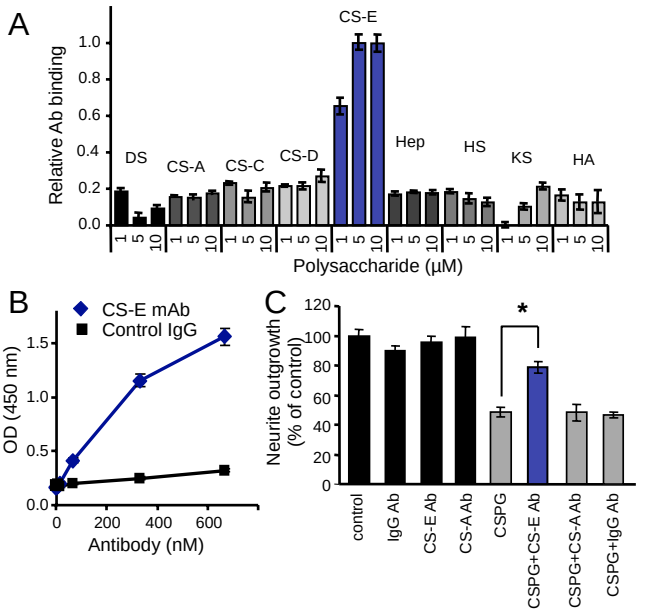

Fig. 4. A monoclonal antibody binds specifically to CS-E and blocks CSPG-mediated neurite inhibition. (*A*) Binding of the CS-E antibody to carbohydrate microarrays. Little binding to other sulfated CS polysaccharides or glycosaminoglycan classes was detected. Experiments were performed in triplicate ($n = 10$ per condition). (*B*) Dose-dependent binding of the anti-CS-E antibody to CSPGs, as shown by an enzyme-linked immunosorbent assay. The experiment was performed in triplicate, and average values (±SD, error bars) are shown for one representative experiment. (*C*) The CS-E antibody blocks CSPG-mediated inhibition of neurite outgrowth. Dissociated chick E7 DRGs were cultured on a substratum of P-Orn (control) or CSPGs (0.5 μg/mL) in the presence of the indicated antibodies (0.1 mg/mL) for 12 h. Quantitation from three experiments is shown (One-way ANOVA, $^*P < 0.0001$, relative to CSPG without antibody treatment control; $n = 50$–200 cells per experiment).

Having demonstrated specific blocking of CSPG activity in vitro, we next examined whether the CS-E antibody could promote axon regeneration in vivo. We performed an optic nerve crush injury in mice (31), which causes focal damage and glial scarring in the optic nerve and thus presents an ideal model for evaluating the effects of local application of the CS-E antibody on axon regeneration. Supporting the notion that CS-E is a prominent inhibitory component associated with CSPGs, pronounced upregulation of CS-E was rapidly observed around the lesion site within 1 d after the injury (Fig. 5*A*). To examine the effects of the CS-E antibody on axon regeneration, gelfoam soaked in a solution containing the CS-E or control IgG antibody was placed around the crush site of the nerve immediately after the injury and replaced twice at day three and six. The extent of axonal regrowth was assessed 2 weeks after injury by anterograde axon tracing with choleratoxin-B subunit (CTB), which was injected intravitreally 3 d before mice were killed. Little axon regeneration was observed in the control antibody-treated group. In contrast, the CS-E antibody treatment resulted in substantial axonal regrowth, with a sixfold increase in the number of regenerating axons when counted at 0.25 mm beyond the injury site, as compared with control antibody-treated mice (Fig. 5*B*). Notably, the extent of axon regeneration observed after CS-E antibody treatment was comparable to that seen in mice treated with ChABC alone (50 U/mL) or with ChABC and CS-E antibody applied simultaneously (50 U/mL and 1.7 mg/mL, respectively). Thus, blockade of CS-E activity induced a similar extent of axon regeneration as

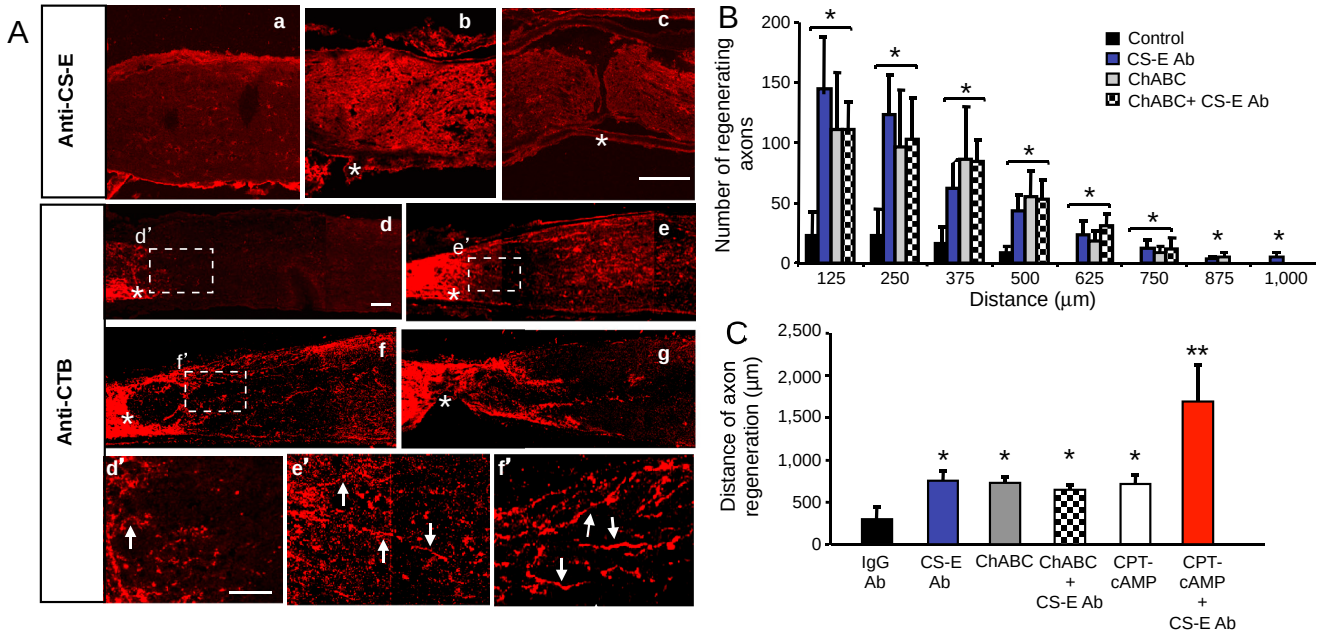

Fig. 5. CS-E neutralizing antibodies promote optic nerve regeneration. (*A*) a–c: Immunofluorescence labeling of CS-E expression in optic nerve sections at day 1 sham-operation (a), optic nerve crush injury (b), or optic nerve crush injury plus ChABC treatment (c). Note upregulation of CS-E around the injury site (b) that was removed by ChABC treatment (c). d–g: Representative epifluorescence photomicrographs of optic nerve sections taken from mice treated with control IgG (d), CS-E antibody (e), ChABC (f) or ChABC plus CS-E antibody (g). Asterisk indicates the crush site. Retinal ganglion cell axons (red) are labeled by an anterograde axon tracer, CTB, which was injected into the vitreous 3 d prior to scarify, followed by immunostaining with goat-anti-CTB antibody. In control antibody-treated mice (d), few regenerating axons are evident. In contrast, numerous regenerating axons were seen extending pass the crush site in CS-E antibody, ChABC or the combine-treated groups (e–g). Scale bars: 75 μm (a–g); 25 μm (d′–f′). Arrowheads indicate regenerating RGC axons. (*B*) Quantification of axon regeneration in vivo. Nerve fibers were counted at 125-μm intervals from the crush site from three nonconsecutive sections, and the number of fibers at a given distance was calculated (±SEM, error bars). Both the anti-CS-E-and ChABC-treated groups showed significantly more regenerating axons as compared with the control IgG antibody-treated group (ANOVA with Bonferroni posttests at each distance, $*P < 0.001$ as compared to controls; $n = 6$ for each group). (*C*) Quantification of the distances of axon regeneration. Longest distance of axon regeneration was measured from at least four nonconsecutive optic nerve sections from each mouse (±SEM, error bars). Combined treatment of CS-E mAb and CPT-cAMP more than tripled the distance of axon regeneration but did not affect the number of regenerating axons compared to the anti-CS-E or CPT-cAMP treatment alone (Fig. S13).

removal of CS chains from the CSPGs, underscoring the inhibitory potency of CS-E in vivo. To rule out the possibility that the observed axon regrowth after CS-E antibody treatment was simply due to improved cell survival, we stained retinal sections with an anti-βIII-tubulin antibody to image retinal ganglion cells and counted the number of surviving cells. No detectable increase in retinal ganglion cell survival was found in the CS-E antibody-treated mice, as compared with control antibody-treated mice (Fig. S13). Remarkably, these results indicate that the complex process of CSPG-mediated neuronal inhibition can be broken down into discrete, active components, which when blocked are sufficient to promote axonal regeneration in vivo.

Combining the CS-E Blocking Antibody with Other Treatments. The failure of axons to regenerate has been attributed to inhibitory molecules in the extrinsic environment and a reduced intrinsic regenerative capacity of mature CNS neurons (1, 2). We therefore examined the ability of the CS-E antibody to enhance axon regrowth in vivo when used in combination with 8-(4-chlorophenylthio)-cyclic AMP (CPT-cAMP), a cAMP analog known to penetrate the cell membrane and activate the intrinsic growth state of neurons (32). In agreement with stimulation of the growth potential of retinal ganglion cell axons, treatment of CPT-cAMP increased the number of regenerating axons by 12-fold compared to the control treated group (Fig. S13). Combined delivery of the CS-E antibody and CPT-cAMP stimulated longer axonal regrowth than either drug treatment alone, increasing the distance of regeneration by more than 3-fold (Fig. 5*C*). The number of regenerating axons compared to the CPT-cAMP treatment alone was not affected (Fig. S13), further supporting the notion that CS-E contributes to the environmental inhibition, but not the intrinsic growth status, of retinal ganglion cell axons. These results demonstrate the potential of combining the CS-E antibody to block inhibitory CSPGs in the extracellular matrix with growth-promoting treatments to enhance the regenerative outcome.

Conclusions

It has long been recognized that CSPGs are one of the major inhibitors of axon regeneration, but until recently, the structural determinants and mechanisms underlying their activity have been poorly understood. In particular, the precise role of the CS sugars and the importance of specific sulfation motifs have been unclear, limiting the development of molecular approaches to counteract CSPGs. Our studies identify a sugar epitope on CSPGs that is primarily responsible for the inhibitory effects of CSPGs. We show that the CS-E motif interacts directly with the PTPσ receptor and activates signaling pathways involved in inhibiting axon growth. These findings defy the conventional view that CSPGs function primarily as a mechanical barrier to axon regrowth (12) and that chondroitin sulfate sugars play nonspecific, passive roles. The ability to upregulate particular sulfated epitopes on the sugar side chains may be essential for regulating CSPG activity by allowing for more precise control beyond mere expression of the core protein. Further, the concerted expression of diverse sulfated epitopes on different CSPGs could provide an elegant mechanism to coordinate the activities of various proteoglycan core proteins.

These studies also provide a potential strategy for promoting axon regeneration and neural plasticity after injury. We show that CS-E blocking strategies can increase axon regeneration in vivo and can be combined effectively with other treatments, such as stimulation of neuronal growth, to further improve the regenerative outcome. Previous studies have demonstrated that antibodies

delivered to the spinal cord can improve function after spinal cord injury (33, 34), and new techniques may even allow antibodies into the brain for the treatment of neurodegenerative diseases (35, 36). Additionally, the development of small-molecule antagonists of CS-E function should also be feasible by inhibiting the sulfotransferase Chst15. Targeting specific CS sugar epitopes using antibodies, small molecules, or other approaches may offer fewer undesirable side effects and a more stable, selective, and less immunogenic alternative to chondroitinase ABC, which is currently being evaluated as a therapeutic treatment for spinal cord injury. Given that CS-E appears to interact with multiple protein receptors and activate multiple signaling pathways, strategies that block the sulfated CS-E epitope may also prove more effective at neutralizing CSPGs than targeting individual CSPG receptors or pathways.

More broadly, our results demonstrate the importance of the fine structure of CS chains in modulating the activity of CSPGs in vivo. In contrast to heparan sulfate, where a handful of important sequences have been identified (17), much less is known about the roles of CS sulfation. We provide in vivo evidence that a specific CS-E sulfation motif within CS polysaccharides signals through protein receptors so as to direct important physiological responses. Our studies underscore the power of synthetic chemistry to deliver sulfated sequences with precise spacing and orientation to assess an underappreciated component of the mechanism. Given the importance of glycosaminoglycans in processes ranging from development to viral invasion and spinal cord injury, an expanded view of these sulfated sugars may provide new insights into many critical biological processes.

Methods

For a detailed description of the materials and methods used, see *SI Methods*.

Neurite Outgrowth Assays. E7 chick DRGs or P5-9 rat CGNs were grown on coverslips coated with poly-DL-ornithine, followed by CS-A, -C, -E polysaccharides or glycopolymers, CSPGs, ChABC-digested CSPGs, or PBS control. For the signaling pathway inhibitor studies, inhibitors against EGFR (AG1478, 15 nM), ROCK (Y27632, 5 μM), and JNK (JNK Inhibitor II, 10 μM) were added in solution at the start of culturing. For inhibition studies using neurons from $PTP\sigma^{-/-}\Delta$ mice, DRGs from adult KO mice or WT controls were grown on laminin-coated plates. Neurons were immunostained with an anti-βIII tubulin antibody, and neurite outgrowth was quantified using NIH software Image J or MetaMorph software. Statistical analysis was performed using the one-way ANOVA; $n = 50$–500 cells per experiment, and results from at least three independent experiments were reported. Further details can be found in *SI Methods*.

Optic Nerve Regeneration Assay. Immediately after crush injury in the optic nerve of adult mice, gelfoam soaked in a solution containing control IgG, CS-E antibody, or ChABC plus CS-E antibody was placed around the crush site. Other groups of mice received an intravitreal injection of CPT-cAMP alone or CPT-cAMP plus CS-E antibody. To label retinal ganglion cell axons, a solution containing the anterograde axon tracer CTB was injected intravitreally 3 d before mice were killed. The extent of axonal regrowth was assessed 2 weeks after injury. For immunofluorescence labeling, sectioned optic nerve and retinal tissue was immunostained with anti-CS-E, anti-CTB, or anti-βIII-tubulin antibodies. To quantify the number of CTB-positive regenerating axons, the number of regenerating axons was counted at 125 μm stepwise from the crush site of the optic nerve. Further details can be found in *SI Methods*.

ACKNOWLEDGMENTS. We thank J. Vielmetter, Director of the Caltech Protein Expression Center, for assistance with the surface plasmon resonance analysis, I. Antoshechkin and the Caltech Millard and Muriel Jacobs Genetics and Genomics Laboratory for printing of the polysaccharide microarrays, and P. Clark for helpful comments on the manuscript. This research was supported by National Institutes of Health grants R01 GM093627-03 (L.H.W.) and 5T32 GM07616-30S1 (J.M.B.), the Roman Reed Spinal Cord Injury Research Fund of California (L.H.W.), and a Christopher & Dana Reeve Foundation Individual Research Grant (B.Z.).

1. Yiu G, He Z (2006) Glial inhibition of CNS axon regeneration. *Nat Rev Neurosci* 7:617–627.
2. Busch SA, Silver J (2007) The role of extracellular matrix in CNS regeneration. *Curr Opin Neurobiol* 17:120–127.
3. Carulli D, Laabs T, Geller HM, Fawcett JW (2005) Chondroitin sulfate proteoglycans in neural development and regeneration. *Curr Opin Neurobiol* 15:116–120.
4. Pizzorusso T, et al. (2006) Structural and functional recovery from early monocular deprivation in adult rats. *Proc Natl Acad Sci USA* 103:8517–8522.
5. Cafferty WB, et al. (2008) Chondroitinase ABC-mediated plasticity of spinal sensory function. *J Neurosci* 28:11998–12009.
6. Bradbury EJ, et al. (2002) Chondroitinase ABC promotes functional recovery after spinal cord injury. *Nature* 416:636–640.
7. Gilbert RJ, et al. (2005) CS-4,6 is differentially upregulated in glial scar and is a potent inhibitor of neurite extension. *Mol Cell Neurosci* 29:545–558.
8. Wang H, et al. (2008) Chondroitin-4-sulfation negatively regulates axonal guidance and growth. *J Cell Sci* 121:3083–3091.
9. Properzi F, et al. (2005) Chondroitin 6-sulphate synthesis is up-regulated in injured CNS, induced by injury-related cytokines and enhanced in axon-growth inhibitory glia. *Eur J Neurosci* 21:378–390.
10. Kitagawa H, Tsutsumi K, Tone Y, Sugahara K (1997) Developmental regulation of the sulfation profile of chondroitin sulfate chains in the chicken embryo brain. *J Biol Chem* 272:31377–31381.
11. Lin R, Rosahl TW, Whiting PJ, Fawcett JW, Kwok JCF (2011) 6-Sulphated chondroitins have a positive influence on axonal regeneration. *Plos One* 6:e21499.
12. Olson L (2002) Medicine: clearing a path for nerve growth. *Nature* 416:589–590.
13. Mckeon RJ, Hoke A, Silver J (1995) Injury-induced proteoglycans inhibit the potential for laminin-mediated axon growth on astrocytic scars. *Exp Neurol* 136:32–43.
14. Sivasankaran R, et al. (2004) PKC mediates inhibitory effects of myelin and chondroitin sulfate proteoglycans on axonal regeneration. *Nat Neurosci* 7:261–268.
15. Kaneko M, Kubo T, Hata K, Yamaguchi A, Yamashita T (2007) Repulsion of cerebellar granule neurons by chondroitin sulfate proteoglycans is mediated by MAPK pathway. *Neurosci Lett* 423:62–67.
16. Tom VJ, Steinmetz MP, Miller JH, Doller CM, Silver J (2004) Studies on the development and behavior of the dystrophic growth cone, the hallmark of regeneration failure, in an in vitro model of the glial scar and after spinal cord injury. *J Neurosci* 24:6531–6539.
17. Bishop JR, Schuksz M, Esko JD (2007) Heparan sulphate proteoglycans fine-tune mammalian physiology. *Nature* 446:1030–1037.
18. Rawat M, Gama CI, Matson JB, Hsieh-Wilson LC (2008) Neuroactive chondroitin sulfate glycomimetics. *J Am Chem Soc* 130:2959–2961.
19. Gama CI, et al. (2006) Sulfation patterns of glycosaminoglycans encode molecular recognition and activity. *Nat Chem Biol* 2:467–473.
20. Ohtake-Niimi S, et al. (2010) Mice deficient in N-acetylgalactosamine 4-sulfate 6-o-sulfotransferase are unable to synthesize chondroitin/dermatan sulfate containing N-acetylgalactosamine 4,6-bissulfate residues and exhibit decreased protease activity in bone marrow-derived mast cells. *J Biol Chem* 285:20793–20805.
21. Aricescu AR, McKinnell IW, Halfter W, Stoker AW (2002) Heparan sulfate proteoglycans are ligands for receptor protein tyrosine phosphatase sigma. *Mol Cell Biol* 22:1881–1892.
22. Shen YJ, et al. (2009) PTP sigma Is a Receptor for Chondroitin Sulfate Proteoglycan, an Inhibitor of Neural Regeneration. *Science* 326:592–596.
23. Sapieha PS, et al. (2005) Receptor protein tyrosine phosphatase sigma inhibits axon regrowth in the adult injured CNS. *Mol Cell Neurosci* 28:625–635.
24. Thompson KM, et al. (2003) Receptor protein tyrosine phosphatase sigma inhibits axonal regeneration and the rate of axon extension. *Mol Cell Neurosci* 23:681–692.
25. McLean J, Batt J, Doering LC, Rotin D, Bain JR (2002) Enhanced rate of nerve regeneration and directional errors after sciatic nerve injury in receptor protein tyrosine phosphatase sigma knock-out mice. *J Neurosci* 22:5481–5491.
26. Rogers CJ, et al. (2011) Elucidating glycosaminoglycan-protein-protein interactions using carbohydrate microarray and computational approaches. *Proc Natl Acad Sci USA* 108:9747–9752.
27. Fisher D, et al. (2011) Leukocyte common antigen-related phosphatase is a functional receptor for chondroitin sulfate proteoglycan axon growth inhibitors. *J Neurosci* 31:14051–14066.
28. Tully SE, Rawat M, Hsieh-Wilson LC (2006) Discovery of a TNF-alpha antagonist using chondroitin sulfate microarrays. *J Am Chem Soc* 128:7740–7741.
29. Clement AM, et al. (1998) The DSD-1 carbohydrate epitope depends on sulfation, correlates with chondroitin sulfate D motifs, and is sufficient to promote neurite outgrowth. *J Biol Chem* 273:28444–28453.
30. Pothacharoen P, et al. (2007) Two related but distinct chondroitin sulfate mimetope octasaccharide sequences recognized by monoclonal antibody WF6. *J Biol Chem* 282:35232–35246.
31. Park KK, et al. (2008) Promoting axon regeneration in the adult CNS by modulation of the PTEN/mTOR pathway. *Science* 322:963–966.
32. Cui Q, Yip HK, Zhao RC, So KF, Harvey AR (2003) Intraocular elevation of cyclic AMP potentiates ciliary neurotrophic factor-induced regeneration of adult rat retinal ganglion cell axons. *Mol Cell Neurosci* 22:49–61.
33. Geremia NM, et al. (2012) CD11d antibody treatment improves recovery in spinal cord-injured mice. *J Neurotrauma*, 29 pp:539–550.
34. Liebscher T, et al. (2005) Nogo-A antibody improves regeneration and locomotion of spinal cord-injured rats. *Ann Neurol* 58:706–719.
35. Yu YJ, et al. (2011) Boosting brain uptake of a therapeutic antibody by reducing its affinity for a transcytosis target. *Sci Transl Med* 3:84ra44.
36. Atwal JK, et al. (2011) A therapeutic antibody targeting BACE1 inhibits amyloid-beta production in vivo. *Sci Transl Med* 3:84ra43.

Supporting Information

Brown et al. 10.1073/pnas.1121318109

SI Text

SI Methods. ***Neurite outgrowth assays.*** Glass coverslips were coated with poly-DL-ornithine (P-Orn) in pH 8.5 borate buffer (0.5 mg/mL) for 2 h at 37 °C and 5% CO_2, followed by CS-A,-C,-E polysaccharides (Seikagaku), CSPGs derived from chick brains (Millipore), digested CSPGs treated with ChABC (Seikagaku; 4 mU ChABC per μg CSPG), or synthesized polymers (1) [polysaccharides and polymers at 1 μg/mL based on uronic acid content (2) in phosphate buffered saline (PBS; 1 mM KH2PO4, 155 mM NaCl, 3 mM Na2HPO4, pH 7.4)] for 2 h at 37 °C and 5% CO_2. For mixed polymer assays, the polymers were mixed at the given concentrations immediately prior to coating. DRGs were dissected from day 7 chick embryos, incubated in 0.125% trypsin w/ EDTA (Invitrogen) for 15 min at 37 °C, triturated to dissociate to single cell suspensions, and grown on the coverslips coated with the above-mentioned substrata. Cells were grown in a growth medium composed of DMEM/F12, 10% horse serum, 50 ng/mL NGF (Sigma-Aldrich), and Insulin-Transferrin-Selenium-X Supplement (Invitrogen) for 12 h. For CGNs, cerebella were dissected from P5-9 Sprague Dawley rats, incubated in 0.125% trypsin w/ EDTA for 15 min at 37 °C, triturated to dissociate to single cell suspensions, and purified on discontinuous 35%–60% Percoll gradient. For the signaling pathway inhibitor studies, inhibitors against EGFR (AG1478, 15 nM; Calbiochem), ROCK (Y27632, 5 μM; Calbiochem), and JNK (JNK Inhibitor II, 10 μM; Calbiochem) were added in solution at the start of culturing, and neurons were grown for 24 h in DMEM/F12, 1% FBS, and N1 supplement at 37 °C and 5% CO_2. For the antibody blocking studies, anti-CS-E, anti-CS-A (Seikagaku), or IgG control antibodies (0.1 mg/mL) were added at the start of culturing to chick E7 DRGs, which were cultured as described above on glass slides with a substratum of P-Orn or CSPGs (0.5 μg/mL) for 12 h.

For inhibition studies using CSPGs derived from *Chst*15$^{-/-}$ mice (34), 96-well Poly-D-Lysine Cellware Plates (BD BioCoat™) were coated with CSPGs in PBS overnight at 37 °C and 10% CO_2. The plates were then washed with PBS and coated with laminin (Invitrogen; 10 μg/mL) in Neurobasal medium (Invitrogen) for 2 h at 37 °C and 10% CO_2. DRGs were dissected from P8 wild-type (WT) mouse pups, incubated in 0.125% trypsin w/ EDTA for 15 min at 37 °C, followed by collagenase (Worthington; 4 mg/mL) for 15 min at 37 °C, triturated to dissociate to single cell suspensions, filtered using a 40-μm cell strainer (Fisher) to remove nondissociated cells, and seeded at approximately 2,000 cells per well. Cells were cultured for 2 d in Neurobasal medium supplemented with B27 and GlutaMAX™ (Invitrogen).

For inhibition studies using neurons from *PTPσ*$^{-/-}$ mice (4), Poly-D-Lysine Cellware Plates were coated with laminin (10 μg/mL) in Neurobasal medium for 2 h at 37 °C and 10% CO_2. DRGs were dissected from adult knockout (KO) mice or WT controls, dissociated, and cultured as described above. CS-E was biotinylated as described (5) and conjugated to streptavidin agarose beads (200 μg of CS in 400 μL PBS incubated with 100 μL agarose resin for 1 h at RT), which were then coplated with the cells (5 μg of 50% slurry per well). Unconjugated beads at the same concentration were used as a control. Cells were grown in Neurobasal medium supplemented with B27 and GlutaMAX™ for 2 d. For all neurite outgrowth experiments, we performed statistical analysis using the one-way ANOVA (n = 50–200 cells per experiment), and results from at least three independent experiments were reported.

Growth cone collapse assays. DRG explants were dissected from E7-9 chick embryos and grown in DMEM/F12 medium supplemented with horse serum (10%), Insulin-Transferrin-Selenium-G Supplement, and NGF (50 ng/mL) on 8-well Lab-Tek® II CC2™ Slides (Electron Microscopy Sciences) that were coated with P-Orn in pH 8.5 borate buffer, followed by laminin (10 μg/mL) in PBS for 2 h at 37 °C and 5% CO_2. CGN explants were dissected from P7-9 rats, chopped with a razor blade into approximately 1-mm^2 pieces, and cultured on P-Orn-coated glass coverslips in DMEM/F12 medium supplemented with 10% horse serum, 5% FBS, and N1 supplement. After 24 h, explants were treated with the indicated polysaccharides or glycopolymers (10 μg/mL based on uronic acid content in media; initial stock 200 μg/mL in PBS) for 30 min. P-values were determined using one-way ANOVA (n = 50–100 growth cones per experiment), and results from at least five independent experiments were reported.

Boundary assays. CS polysaccharides (1 mg/mL based on uronic acid content) were mixed with Texas Red (0.5 mg/mL; Invitrogen) in PBS, spotted at the center of P-Orn-coated coverslips (5 μL), and incubated for 2 h at 37 °C and 5% CO_2. Cerebella were dissected from P5-9 Sprague Dawley rats, incubated in 0.125% trypsin w/ EDTA for 15 min at 37 °C, triturated to dissociate to single cell suspensions, and purified on a discontinuous 35%–60% Percoll gradient. These cells were then cultured on the coated coverslips for 48 h. After immunostaining for neurite outgrowth, axons growing toward the boundary and within 10 μm distance of the boundary were evaluated. The percentage of axons that crossed the boundary over the total axons was quantified. P-values were determined using one-way ANOVA (n = 30–50 axons per experiment) and results from two independent experiments were reported.

Immunostaining and quantification. All neuronal cultures were fixed with paraformaldehyde, permabilized with 0.1% Triton X-100 in PBS, blocked with 1% BSA in PBS, and incubated with a mouse anti-βIII tubulin antibody (Sigma) overnight at 4 °C, followed by an Alexa Fluor 488-conjugated goat anti-mouse IgG secondary antibody (Invitrogen) for 1–2 h at room temperature for neurite outgrowth and boundary assays, or by rhodamine phalloidin (Pierce) for 1 h at room temperature for growth cone collapse assays. Cells were imaged using a Nikon TE2000-S fluorescent microscope or Zeiss LSM Pascal, and neurite outgrowth was quantified using NIH software Image J or MetaMorph software. Statistical analysis was performed using the one-way ANOVA (n = 50–500 cells per experiment), and results from at least three independent experiments were reported.

Protein expression and binding assays. For pull-down assays, full-length mouse *PTPσ* (Open Biosystems) was ligated into a pcDNA vector (Invitrogen) modified to fuse a myc-His tag to the 5′ end of the insert. COS-7 cells were transfected using Lipofectamine (Invitrogen) and lysed 2 d after transfection with 1% Triton X -100 in PBS containing a protease inhibitor cocktail (Roche). Lysates were then incubated with streptavidin agarose resin (Pierce; 30 μL) with end-over-end mixing for 1 h at 4 °C to reduce nonspecific binding. The supernatant was collected, added to 30 μL of either CS-C or CS-E streptavidin agarose resin, and incubated with end-over-end mixing for 4 h at 4 °C. The supernatant was removed, and the resin was washed three times with PBS (500 μL). Resin was boiled with 2X loading dye (30 μL of 100 mM Tris, 200 mM DTT, 4% SDS, 0.10% bromophenol blue,

20% glycerol), and the eluate was resolved by SDS-PAGE and transferred to PVDF membrane. PTPσ-myc was detected by immunoblotting with an anti-myc antibody (Cell Signaling) following the manufacturer's protocol. For ELISA and microarray assays, the extracellular domain of PTPσ was ligated into a pcDNA vector that had been modified to append a human Fc domain and myc-His tag to the expressed protein. HEK293T cells were transfected using Lipofectamine, and the conditioned media was collected and used for ELISA or subjected to Ni-NTA agarose purification for carbohydrate microarray assays.

ELISA and dot blot assays. To assay for PTPσ binding, PTPσ-Fc was incubated in 96-well protein A-coated plates (Pierce) overnight at 4 °C. The plates were washed with PBS containing 0.05% Tween-20 (PBST) and then incubated with biotinylated CS-A, CS-C, or CS-E polysaccharides in PBS for 2 h at room temperature. For the antibody blocking study, biotinylated CS-E (10 nM in PBS) was preincubated with the CS-C antibody (6) or CS-E antibody (10 μM) for 1 h at RT. The plates were then blocked with 1% BSA in PBS for 30 min at room temperature, incubated with horseradish peroxidase-conjugated streptavidin (Pierce; 1:25,000) for 1 h, and developed with TMB substrate (3,3′,5,5′-tetramethylbenzidine; Pierce) for 20 min and quenched with 2 M H_2SO_4. The absorbance at 450 nm was recorded on a PerkinElmer Victor plate reader. Experiments were performed in triplicate, and data represent the mean ± SEM, error bars.

For CS-E antibody binding to CSPGs, CSPGs (10 μg/mL; 25 μL) were incubated in a Nunc Maxisorp 384-well plate for 2 h. After blocking with 3% BSA in PBS, the anti-CS-E antibody (at the indicated concentrations in 1% BSA in PBS) was incubated in each well for 2 h. For CS binding assays, streptavidin (20 μg/mL; 50 μL) was absorbed in each well for 1 h, followed with biotinylated CS (20 μg/mL; 50 μL) for 1 h. After blocking with 3% BSA in PBS, the anti-CS-E antibody (25 μL of 20 μg/mL or indicated concentrations in 1% BSA in PBS) was incubated in each well for 2 h. Following incubation with horseradish peroxidase-conjugated anti-mouse IgG secondary antibody, the plates were developed and analyzed as described above. Dot blot assays for binding of CS-E Ab to CS polysaccharides were performed as described previously (7).

Microarray assays. Microarrays were generated as described previously (8). Arrays were blocked with 10% FBS in PBS with gentle rocking at 37 °C for 1 h, followed by a brief rinse with PBS. PTPσ-Fc, EphA2-Fc (R & D Systems), or Fc was reconstituted in 1% BSA in PBS, added to the slides in 100 μL quantities at a concentration of 1 μM, and incubated at room temperature for 3 h. The slides were briefly rinsed three times with PBS, and then incubated with a goat anti-human IgG antibody conjugated to Cy3 (Jackson ImmunoResearch; 1:5,000 in PBS) for 1 h in the dark with gentle rocking, and scanned at 532 nm using a GenePix 5000a scanner. Fluorescence quantification was performed using GenePix 6.0 software (Molecular Devices). Binding of the CS-E antibody was evaluated using 100 μL of a 1 μg/mL (or approximately 7 nM) solution of antibody and a goat anti-mouse IgG secondary antibody conjugated to Cy3. Experiments were performed in triplicate, and the data represent the average of 10 spots per concentration averaged from the three experiments (±SEM, error bars).

Mass spectrometry analysis. Brains were dissected from P7-P9 Sprague Dawley rats, homogenized in 0.32 M sucrose with protease inhibitors (Roche), and centrifuged at 1,000 × *g* for 10 min. The supernatant was collected, and then centrifuged at 10,000 × *g* for 20 min. The pellet was discarded, and the supernatant was centrifuged again at 12,000 × *g* for 30 min. This supernatant was then ultracentrifuged at 200,000 × *g* for 1 h, and the pellet was saved and homogenized again in 0.32 M sucrose with protease inhibitors. The supernatant was again ultracentrifuged at 200,000 × *g* for 1 h and the pellet was saved, solubilized in 1% Triton X-100 (PBST) with protease inhibitors, and centrifuged at 12,000 × *g* for 15 min. The final supernatant was obtained as the membrane protein-enriched fraction and incubated with CS-E or unsulfated CS conjugated to streptavidin agarose resin (described above) overnight at 4 °C. The resin was washed with PBS, and the PBS was collected and measured until the OD_{280} was less than 0.05. The bound proteins were then eluted with PBS containing 500 mM NaCl. The eluted proteins were then dialyzed into PBS and subjected to SDS-PAGE. The resulting gel was stained with Coomassie Brilliant Blue, and the band at 206 kDa was cut out, subjected to tryptic digestion, and analyzed by liquid chromatography-mass spectrometry (LC-MS) analysis as reported (9).

Surface plasmon resonance. All experiments were performed on a Biacore T100 at 25 °C using a Sensor Chip CM5 with a running buffer composed of 0.01 M Hepes, pH 7.4, 0.15 M NaCl, 3 mM EDTA, 0.05% Surfactant P20 (HBS-EP+). To analyze the binding of the CS-E antibody to the CS-E tetrasaccharide, both control and active flow cells were exposed to a 1:1 mixture of *N*-hydroxysuccinimide (NHS) and 1-ethyl-3-(3-dimethylaminopropyl)carbodiimide (EDC) for 3 min at a flow rate of 10 $\mu L \cdot min^{-1}$. Next, 5 mM carbohydrazine was injected at the same flow rate for 7 min. Ligand was covalently attached to the surface by injecting a 0.5 mM solution of synthetic CS-E tetrasaccharide bearing an aldehyde group on a reducing-end linker, prepared as previously described (7), onto the active flow cell briefly at a high flow rate (10 s, 60 $\mu L \cdot min^{-1}$), followed by a 20 min injection of 0.1 M sodium cyanoborohydride in 0.1 M sodium acetate pH 4.0 at 2 $\mu L \cdot min^{-1}$. Because of the low molecular weight of the CS-E tetrasaccharide, it was not possible to observe the amount of ligand bound to the surface. Instead, 500 nM of the CS-E antibody was injected into both the control and active flow cell to test the response. The amount of ligand was increased accordingly until an adequate response was observed. The kinetics of the CS-E antibody/CS-E tetrasaccharide interaction was determined by 300 s injections of the CS-E antibody at 30 $\mu L \cdot min^{-1}$. The dissociation was monitored for 900 s before the surface was regenerated with a 30 s injection of 6 M guanidine HCl. The resulting sensorgrams were fit to the bivalent analyte model. Affinity analysis was measured by injecting the antibody for 3,600 s at 5 $\mu L \cdot min^{-1}$. After 600 s, the surface was regenerated with a 60 s injection at 10 $\mu L \cdot min^{-1}$. The data were analyzed by plotting the response at equilibrium versus concentration and fitting the resulting curve to the Langmuir equation.

CSPG purification. Adult brains from *Chst15* knockout mice or WT controls were dissected and homogenized in PBS with 20 mM EDTA and protease inhibitors (Roche). The homogenates were centrifuged at 27,000 × *g* for 1 h at 4 °C. The supernatant was collected, and the pellet was homogenized and centrifuged as before, and the second supernatant was added to the first (total volume 8 mL). Urea (1 g) was added, and the supernatant was incubated at 4 °C for 1 h. For each brain, 2 mL of DEAE Sephacel beads was added to a column, and the supernatant was incubated with these beads for 2 h at 4 °C. The column was then drained, and washed with 50 mM Tris HCl, pH 7.5, 2 mM EDTA, 2 M urea, 0.25 M NaCl. The CSPGs were eluted with the same buffer, with 0.75 M NaCl. The eluate was concentrated using 50 kDa filter columns (Amicon), and dialyzed into PBS. Protein concentrations were determined using the carbazole assay with commercial CSPGs (Millipore) as a concentration standard.

RhoA activation assay. COS-7 cells were cultured in DMEM supplemented with 10% FBS. The cells were serum starved overnight, and then the medium was removed and replaced with serum-free medium containing CS-E polysaccharides or CSPGs (10 μg/mL). After 10 min, the cells were lysed, and RhoA activation was determined using the G-LISA kit (Cytoskeleton).

Immunostaining of retinal and optic nerve sections. At 14 days post injury, mice were given an overdose of pentobarbital and were transcardially perfused with 4% paraformaldehyde (PFA). Eyeballs still attached with the optic nerve were dissected and post-fixed in 4% PFA overnight. Following cryoprotection with 30% sucrose in PBS, tissues were embedded in Tissue-Tek® OCT™ and serial sectioned for 10 μm along the longitudinal direction of the nerve. For immunofluorescence labeling, the sections were washed with PBS, preincubated in a blocking buffer (1% BSA, 0.3%TX-100 in PBS) and followed by sequential incubations with primary antibodies, including mouse anti-CS-E (1:200), goat-anti-CTB (1:4,000), or rabbit anti-βIII-tubulin antibodies (Invitrogen). The sections were then reacted with biotinylated anti-goat IgG (1:200) and visualized with Alexa Fluor 546-conjugated streptavidin (1:400) or with a Cy3-conjugated goat anti-mouse or -rabbit IgG. The retinal cryosections were mounted with Vectashield and visualized under a Nikon fluorescence microscope. To quantify the number of CTB-positive regenerating axons, the number of regenerating axons was counted at 125 μm stepwise from the crush site of the optic nerve. The total number of regenerating axons was estimated as described (10). To quantify the number of surviving retinal ganglion cells, the total number of βIII-tubulin positive cells was counted in at least 3 retinal sections per retina.

Optic nerve regeneration assay. Immediately after crush injury in the optic nerve of adult mice, gelfoam soaked in a solution containing control IgG, CS-E antibody (1.7 mg/mL), chondroitinase ABC (ChABC; 50 U/mL), or ChABC (50 U/mL) plus CS-E antibody (1.7 mg/mL) was placed around the crush site of the nerve and replaced after three days. To analyze whether CS-E contributes primarily to the growth inhibition associated with CSPGs and acts extrinsic to neurons to block nerve regeneration, we also compared the effects of the CS-E antibody on optic nerve regeneration in vivo with that of CPT-cAMP, which is reported to stimulate the intrinsic growth status of retinal ganglion cell axons. Thus, in other groups of mice, mice that received an intravitreal injection of CPT-cAMP (100 mM, 2 μL) alone or CPT-cAMP plus CS-E antibody (1.7 mg/mL) treatment placed around the crush site of the nerve were studied. To label retinal ganglion cell axons, 2 μL of a solution containing an anterograde axon tracer, CTB, was injected intravitreally 3 d before mice were killed. The extent of axonal regrowth was assessed 2 weeks after injury.

1. Rawat M, Gama CI, Matson JB, Hsieh-Wilson LC (2008) Neuroactive chondroitin sulfate glycomimetics. *J Am Chem Soc* 130:2959–2961.
2. Taylor KA, Buchanan-Smith JG (1992) A colorimetric method for the quantitation of uronic acids and a specific assay for galacturonic acid. *Anal Biochem* 201:190–196.
3. Ohtake-Niimi S, et al. (2010) Mice deficient in N-acetylgalactosamine 4-sulfate 6-O-sulfotransferase are unable to synthesize chondroitin/dermatan sulfate containing N-acetylgalactosamine 4,6-bissulfate residues and exhibit decreased protease activity in bone marrow-derived mast cells. *J Biol Chem* 285:20793–20805.
4. Elchebly M, et al. (1999) Neuroendocrine dysplasia in mice lacking protein tyrosine phosphatase sigma. *Nat Genet* 21:330–333.
5. Saito A, Munakata H (2004) Detection of chondroitin sulfate-binding proteins on the membrane. *Electrophoresis* 25:2452–2460.
6. Gama CI, et al. (2006) Sulfation patterns of glycosaminoglycans encode molecular recognition and activity. *Nat Chem Biol* 2:467–473.
7. Tully SE, Rawat M, Hsieh-Wilson LC (2006) Discovery of a TNF-alpha antagonist using chondroitin sulfate microarrays. *J Am Chem Soc* 128:7740–7741.
8. Rogers CJ, et al. (2011) Elucidating glycosaminoglycan-protein-protein interactions using carbohydrate microarray and computational approaches. *Proc Natl Acad Sci USA* 108:9747–9752.
9. Clark, PM, et al. (2008) Direct in-gel fluoresence detection and cellular imaging of *O*-GlcNAc-modified proteins. *J Am Chem Soc* 130:11576–11577.
10. Leon S, et al. (2000) Lens injury stimulates axon regeneration in the mature rat optic nerve. *J Neurosci* 20:4615-4626.

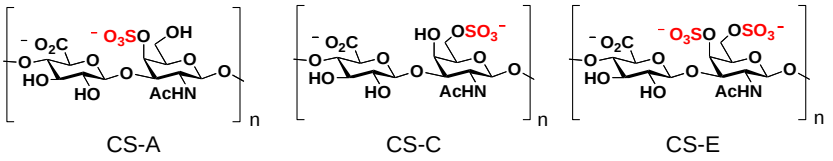

Fig. S1. CS polysaccharides are composed of 20–200 units of the repeating disaccharide D-glucuronic acid (GlcA) and *N*-acetyl-D-galactosamine (GalNAc). The sugar hydroxyls are variably sulfated to give rise to diverse sulfation patterns. Chemical structures of major sulfation motifs found in the mammalian nervous system: CS-A (GlcA-4SGalNAc), CS-C (GlcA-6SGalNAc), and CS-E (GlcA-4S, 6SGalNAc). $n = 20–200$.

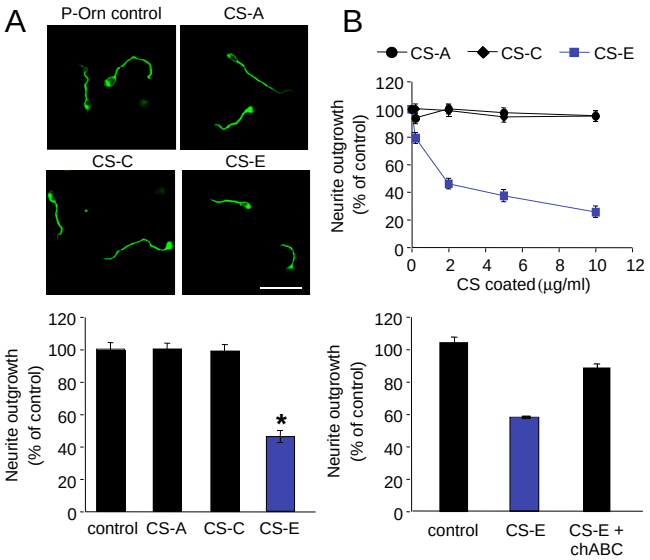

Fig. S2. Polysaccharides enriched in the CS-E sulfation motif (60% CS-E content), but not CS-A or CS-C (90% CS-A and CS-C content, respectively), inhibit the neurite outgrowth of cerebellar granule neurons (CGNs). (*A*) Dissociated P5-9 rat CGNs were cultured on a substratum of polysaccharides enriched in the CS-A, CS-C, or CS-E sulfation motifs (1 μg/mL) for 24 h. Cells were immunostained using an anti-βIII-tubulin antibody, imaged and quantified using the NIH software Image J. Representative images are shown on the top, and quantitation of the average neurite length (±SEM, error bars) from at least three experiments is shown on the bottom (One-way ANOVA, $*P < 0.0001$, relative to P-Orn control; $n = 50–200$ cells per experiment). (*B*) Polysaccharides enriched in the CS-E sulfation motif, but not the CS-A or CS-C motifs, inhibit CGN outgrowth in a dose-dependent manner (*Top*). Chondroitinase ABC (4 mU/μg) digestion abolishes the inhibitory properties of CS-E-enriched polysaccharides (1 μg/mL) in CGNs (*Bottom*).

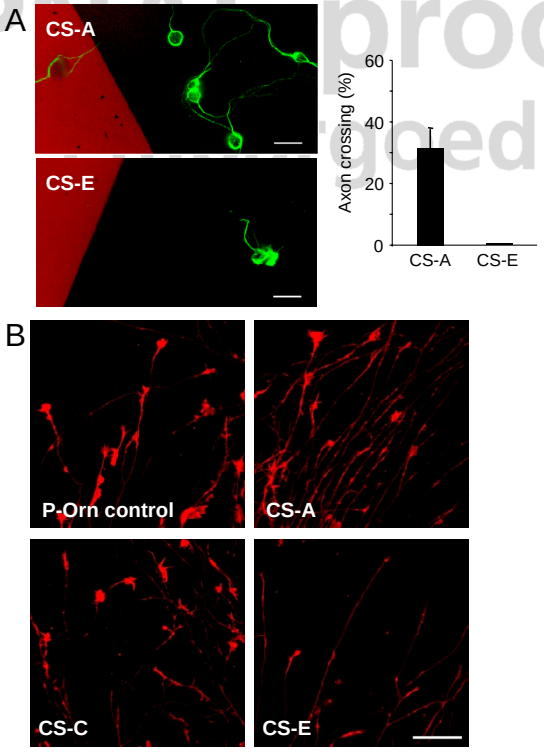

Fig. S3. Representative images of the (*A*) axon repellant activity of CS-A and CS-E polysaccharides at high sugar concentrations (10 mg/mL) and (*B*) growth cone collapse in rat P7-9 CGN explants induced by CS-E polysaccharides. Scale bars, 30 μm.

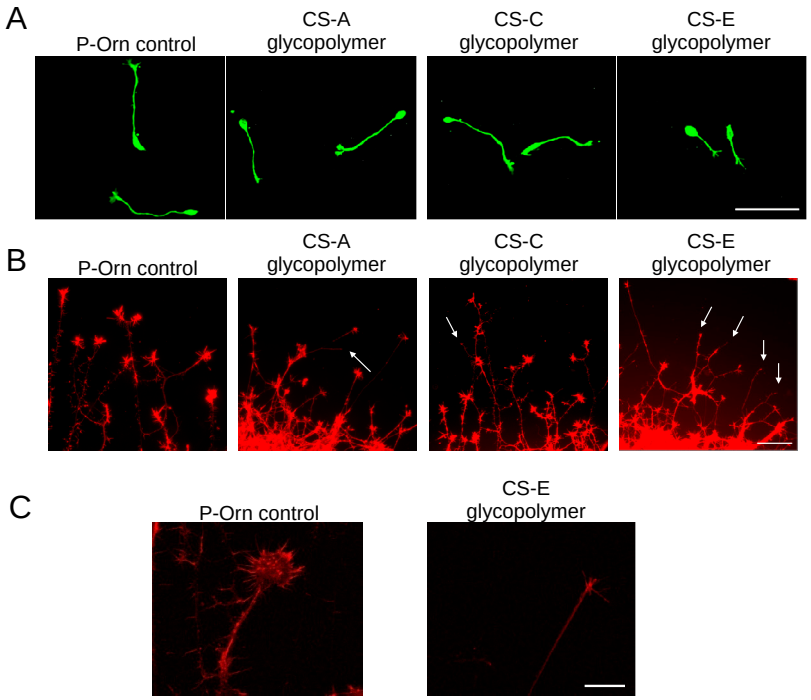

Fig. S4. Representative images of the (*A*) inhibition of chick E7 DRG outgrowth by the synthetic glycopolymers, and (*B*) growth cone collapse of chick E7-9 DRG explants induced by the synthetic glycopolymers. Arrows indicate collapsed growth cones. (*C*) Higher magnification images (60 ×) of intact and collapsed growth cones. Scale bars A and B: 100 μm, C: 20 μm.

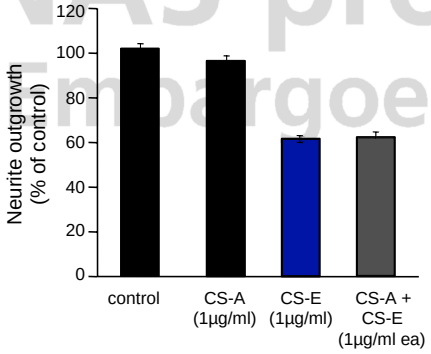

Fig. S5. A mixture of the CS-A and CS-E synthetic glycopolymers does not confer additional inhibitory properties compared to the pure CS-E glycopolymer. Dissociated E7 chick DRGs were cultured on the indicated substrates for 12–14 h. Cells were immunostained using an anti-βIII-tubulin antibody, imaged, and quantified using the NIH software Image J. Quantitation of average neurite length (±SEM, error bars) from three experiments (n = 100–150 cells per experiment) is shown.

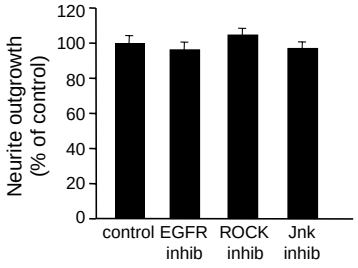

Fig. S6. Inhibitors to EGFR, ROCK, and JNK alone have no effect on CGN outgrowth in the absence of CS-E or CSPGs. Dissociated rat P5-9 CGN neurons were cultured on a P-Orn substratum in the presence or absence of inhibitors against EGFR (AG1478, 15 nM), ROCK (Y27632, 5 μM), and JNK (inhibitor II, 10 μM) for 24 h. Neurites were visualized by staining with an anti-β-tubulin III antibody, and quantitation of neurite outgrowth from at least three independent experiments is shown (n = 50–200 cells per experiment).

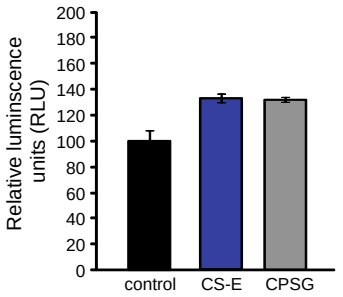

Fig. S7. CS-E and CSPGs activate RhoA. Serum starved COS-7 cells treated with CS-E polysaccharides or CSPGs (10 μg/mL) for 10 min. Cell lysates were standardized for total protein concentration and then added to a 96-well plate containing immobilized rhotekin-RBD, which binds the active (GTP-bound) form of RhoA. Bound RhoA was detected using a RhoA antibody followed by a horseradish peroxidase-labeled secondary antibody. Relative luminescence units (RLU) are plotted relative to that of the untreated control (cell medium alone) for two experiments.

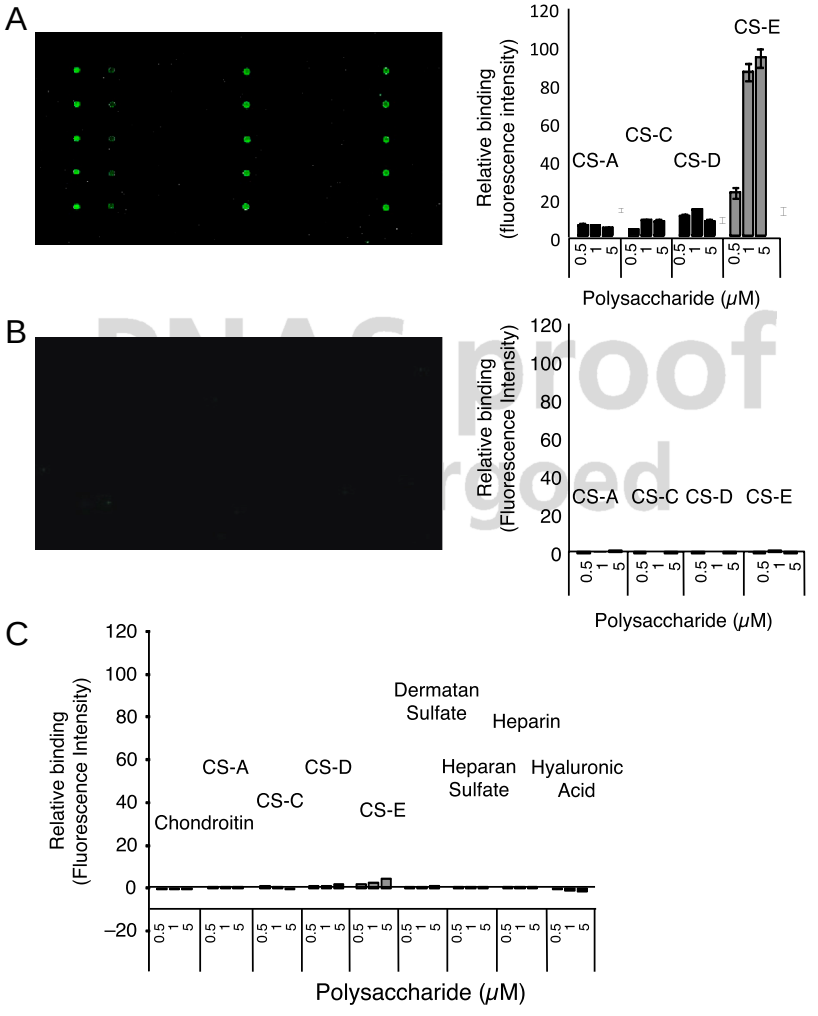

Fig. S8. PTPσ-Fc but not Fc alone or EphA2-Fc bind preferentially to CS-E-enriched polysaccharides. Representative portion of the microarray after binding to PTPσ-Fc (*A*, *Left*) or Fc control (*B*, *Left*). Quantitation from three experiments is shown on the right. Each bar (*A* and *B*, *Right*) represents an average of 10 spots per carbohydrate concentration. (*C*) EphA2-Fc binding to carbohydrate microarrays. Binding relative to PTPs-Fc is shown.

279 PVGRNVLELTDVKDSANYTCV

1074 LTNRGSSLGGLQQTVTARTAF

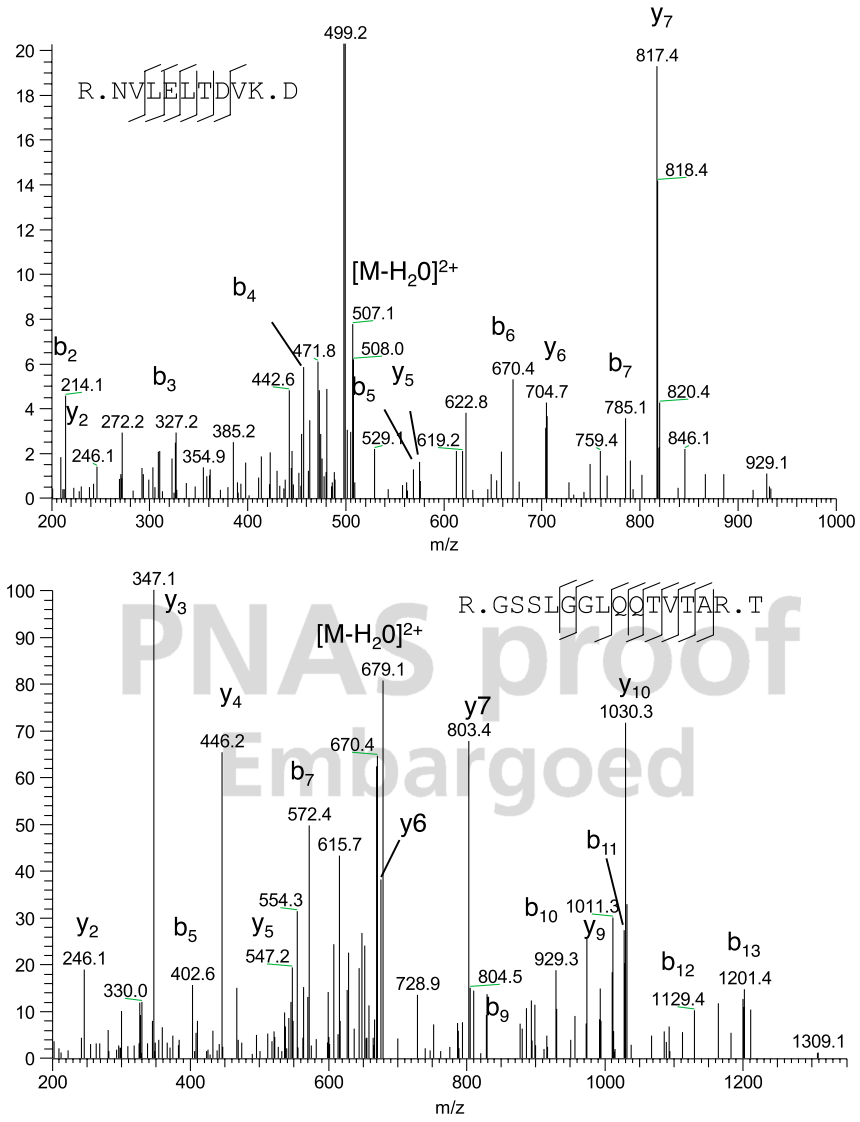

Fig. S9. PTPσ peptides identified by LC-MS/MS analysis. PTPσ from rat brain lysates was pulled down using CS-E and resolved by SDS-PAGE. In-gel tryptic digestion and LC-MS/MS analysis revealed two unique peptides within PTPσ. The annotated spectra from collision-activated dissociation mass spectrometry (CAD-MS) of the peptides show the y and b fragment ions enabling identification.

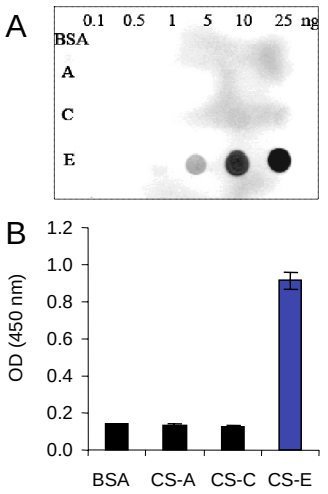

Fig. S10. The anti-CS-E antibody selectively binds to a pure CS-E tetrasaccharide and natural CS-E-enriched polysaccharides, whereas it does not bind to CS-A or CS-C tetrasaccharides or natural polysaccharides. (*A*) Tetrasaccharides containing pure CS-A, CS-C, or CS-E motifs were conjugated to bovine serum albumin (BSA) and spotted on nitrocellulose membranes at the indicated amounts. Binding of the antibody to the membrane was detected using an Alexa Fluor 680-conjugated goat antimouse secondary antibody. The anti-CS-E antibody bound in a concentration-dependent manner to the BSA-CS-E tetrasaccharide conjugate but did not bind significantly to BSA-CS-A, BSA-CS-C, or BSA alone. (*B*) Binding of the anti-CS-E antibody to biotinylated CS polysaccharides enriched in the CS-A, CS-C, or CS-E sulfation motifs. Biotinylated CS polysaccharides were absorbed on streptavidin-coated plates, and antibody binding to the plate was detected using a goat anti-mouse secondary antibody conjugated to horseradish peroxidase. Experiments were repeated in triplicate.

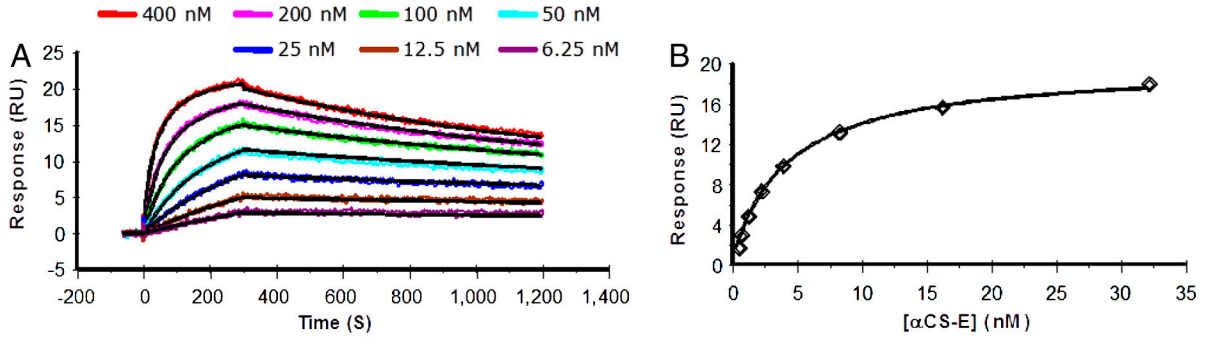

C

k_{a1} ($M^{-1}s^{-1}$)	k_{d1} (s^{-1})	k_{a2} ($RU^{-1}s^{-1}$)	k_{d2} (s^{-1})	R_{max} (RU)	χ^2(RU^2)
3.77 (±0.00) × 10^4	6.41 (±0.01) × 10^{-4}	4.71 (±0.84)	11.9 (±2.1)	22.6 (±0.02)	0.059

Fig. S11. Kinetic analysis of the interaction between the anti-CS-E antibody and CS-E tetrasaccharide by surface plasmon resonance. (*A*) The synthetic CS-E tetrasaccharide was covalently immobilized onto the surface via reductive amination chemistry (see *Materials and Methods*). Kinetics were monitored at 25 °C by injecting the CS-E antibody over the surface for 300 s at 30 μL · min^{-1} and recording the disassociation for 900 s before the surface was regenerated with 6 M guanidine HCl. The resulting sensorgrams were fit to the bivalent analyte model. According to this model, a surface-bound analyte can bind another ligand molecule with the free binding site. The kinetic parameters of the fit, with standard errors in parentheses, are tabulated in (*C*). The affinity was also measured by injecting the antibody over the surface for 3,600 s to give sufficient time to reach equilibrium. The response at equilibrium was plotted versus concentration to give a K_D of 4.3 nM (*B*).

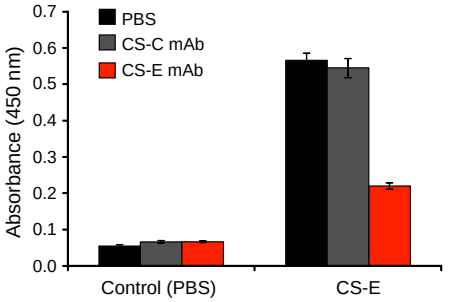

Fig. S12. The CS-E monoclonal antibody (mAb) attenuates binding of CS-E polysaccharides to PTPσ-Fc. PTPσ-Fc was immobilized in protein A-coated 96-well plates. Biotinylated CS-E (10 nM) in PBS was added in the presence of PBS (control), CS-C mAb (10 μM), or CS-E mAb (10 μM). Binding of CS-E was detected using a streptavidin-horseradish peroxidase conjugate. The experiment was performed in duplicate.

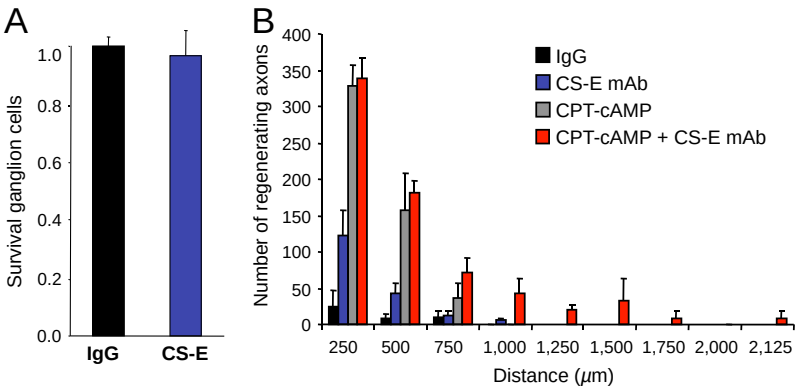

Fig. S13. The CS-E antibody does not affect the survival or intrinsic growth status of retinal ganglion cells. (*A*) Application of the CS-E antibody does not change retinal ganglion cell survival after optic nerve injury. Bar graph indicates relative survival of retinal ganglion cells in control IgG or CS-E antibody treated mice that were quantified at 14 days post optic nerve injury. (*B*) Comparison of axon regeneration in vivo induced by the CS-E antibody and/or CPT-cAMP. Retinal ganglion cell axons were counted at 125-μm intervals from the crush site from three nonconsecutive sections, and the number of fibers at a given distance was calculated as previously described (5) (±SEM, error bars). (ANOVA with Bonferroni posttests at each distance, $*P < 0.001$ as compared to controls; $n = 6$ for each group.

AUTHOR QUERIES

AUTHOR PLEASE ANSWER ALL QUERIES **1**

Q: 1_PNAS prefers the term “killed” to “sacrificed.” The sentence will stand as it appears in the proof.